/

ARGONNE NATIONAL LABORATORY
P. O. Box 299
Lemont, Illinois

INTERACTION OF URANIUM AND ITS ALLOYS WITH CERAMIC OXIDES

by

H. M. Feder, N. R. Chellew, C. L. Rosen

Chemical Engineering Division

July 1957

DISCLAIMER

DISCLAIMER

Portions of this document may be illegible in electronic image products. Images are produced from the best available original document.

TABLE OF CONTENTS

INTERACTION OF URANIUM AND ITS ALLOYS WITH CERAMIC OXIDES
by
H. M. Feder, N. R. Chellew, C. L. Rosen

ABSTRACT

The corrosion of ceramic oxides by molten uranium and its alloys was examined. Dense, high-purity alumina, magnesia, zirconia, beryllia and thoria were studied. The studies included: (a) wettability of ceramics; (b) products of reaction; (c) mechanism of reaction; (d) contamination of molten uranium by crucible material; and (2) the effect of alloying additions on these.

I. INTRODUCTION

This investigation of the interaction of ceramic oxides with molten uranium and its alloys was made primarily for two reasons. First quantitative data on the contamination of uranium due to interactions in ordinary melting and casting practices are of intrinsic interest. Second, these reactions play an important role in the process of melt refining irradiated uranium for the removal of fission products.[1]

The refractory oxides examined were chosen for chemical and physical properties which make them suitable for containing molten uranium. This report includes results obtained with alumina, magnesia, thoria, beryllia, and lime-stabilized zirconia in the temperature range 1140 to 1330 C.

II. EXPERIMENTAL

A. Materials

Ceramics were fabricated from the purest available commercial materials, except for zirconia which contained from five to eight per cent lime for stabilization. Prior to use, the ceramic was subjected to a high-temperature outgassing treatment under less than 1 micron pressure. Bulk densities of the ceramic oxide plaques and crucibles selected for the experiments were: (p = plaque, c = crucible) alumina, 2.68 (p), 2.79 (c); magnesia, 3.25 (p), 2.50 (p), 2.36 (c), 2.79 (c); thoria, 9.55 (p), 5.62 (c); beryllia, 2.03 (p, c); zirconia, 5.29 (p), 3.73 (c).

Biscuit uranium of known purity was used in all experiments. This metal contained maximum concentrations of 39 ppm carbon and 11 ppm oxygen and nitrogen. Previous melting experience had emphasized

the necessity of selecting uranium with limited amounts of carbon, nitrogen and oxygen. These impurities, when present in excess of their solubilities, combine with uranium to form a dross which either liquates or adheres to the container, thereby limiting the value of observations made in a corrosion study.

An inert atmosphere was essential for the studies because the strong gettering property of heated uranium in an impure environment would have permitted confusing side reactions to occur. All experiments were carried out in vacua of less than 0.01 of a micron or in an atmosphere of helium purified by passage through an activated charcoal trap cooled with liquid nitrogen. Analyses for impurities in uranium prior to and after melting in alumina (see Table 1) provided evidence that reactions with impurities in the helium played only a minor role in the experiments.

Table 1

ANALYSES OF URANIUM MELTED IN ALUMINA

Crucible: Morgan Triangle RR recrystallized alumina
Conditions: 1200 C for 2 hr
Atmosphere: Purified helium

| | Composition of Uranium, ppm | | |
| | | After Melting | |
Element	Before Melting	Run 20 E	Run 24 E
Carbon	30	31	50
		30	50
Oxygen	11	16	14
		16	13
Nitrogen	10	14	10
		13	

B.   Equipment and Procedure

Two types of experiments were carried out. In the first, small amounts (approximately 2 grams) of metal were melted to form a sessile drop on a polished ceramic plaque. These experiments yielded information regarding ceramic wettability and the qualitative nature of the reactions. Quantitative data for the same reactions were then obtained by heating approximately 500 grams of material in appropriate ceramic crucibles. Although reaction mechanisms and products were unchanged, the use of larger quantities of materials and the increased areas for reaction were distinct advantages, leading to greater precision in analyses and area measurements.

The assembly used for the sessile drop experiments shown in Figure 1. The induction-heated, horizontally mounted Pyrex tube was similar in design to one used by Humenik and Kingery[2] for surface tension and wettability studies of metal-ceramic systems. Glass flats at each end served as sight ports for photography and optical pyrometry. The inner furnace parts were arranged so that a leveled one-inch square ceramic plaque and metal button placed on it were uniformly heated by a tantalum induction susceptor. Tantalum radiation shields were used to prevent excessive heat loss. Photographs of the sessile drop formed shortly after melting permitted wettability measurements to be made. After additional time at temperature the plaques were cooled to room temperature and sections of the ceramic, reaction layer, and metal were cut for metallographic study and/or chemical analyses of the reaction zones.
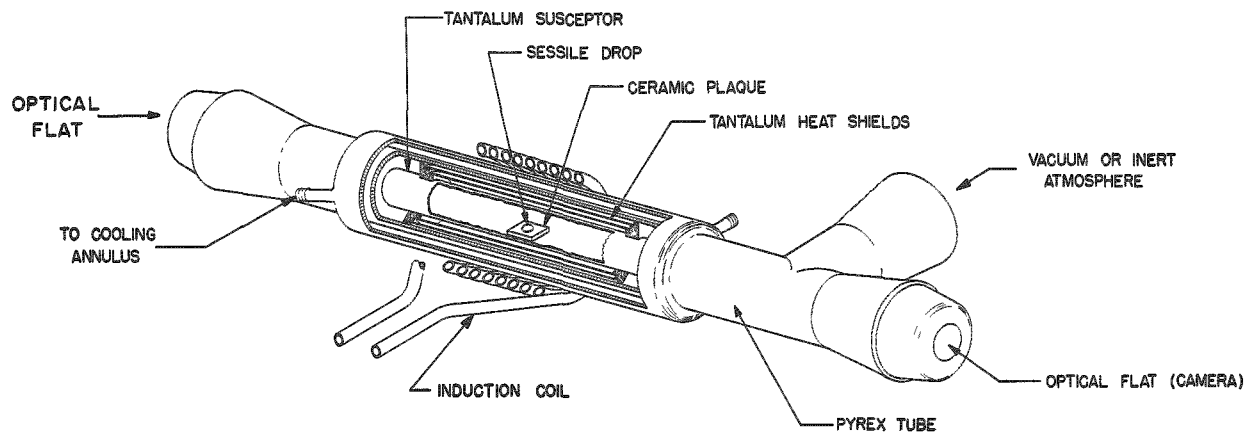
FIGURE 1

FURNACE ASSEMBLY FOR SESSILE DROP STUDIES

Figure 2 shows the equipment employed to study the kinetics of contamination of uranium and its alloys resulting from reaction with ceramics. The furnace was essentially a cylindrical, water-cooled can with a diameter of 20 in. and height of 25 in. The centrally located crucible and heater were surrounded by triple radiation shields. Melt temperatures were determined by an optical pyrometer sighted on the liquid uranium surface, and corrections determined by comparison with the temperature of an immersed, protected Pt-Pt, 10% Rh thermocouple were applied. In order to minimize stirring, molybdenum resistance heating, rather than induction heating, was used.
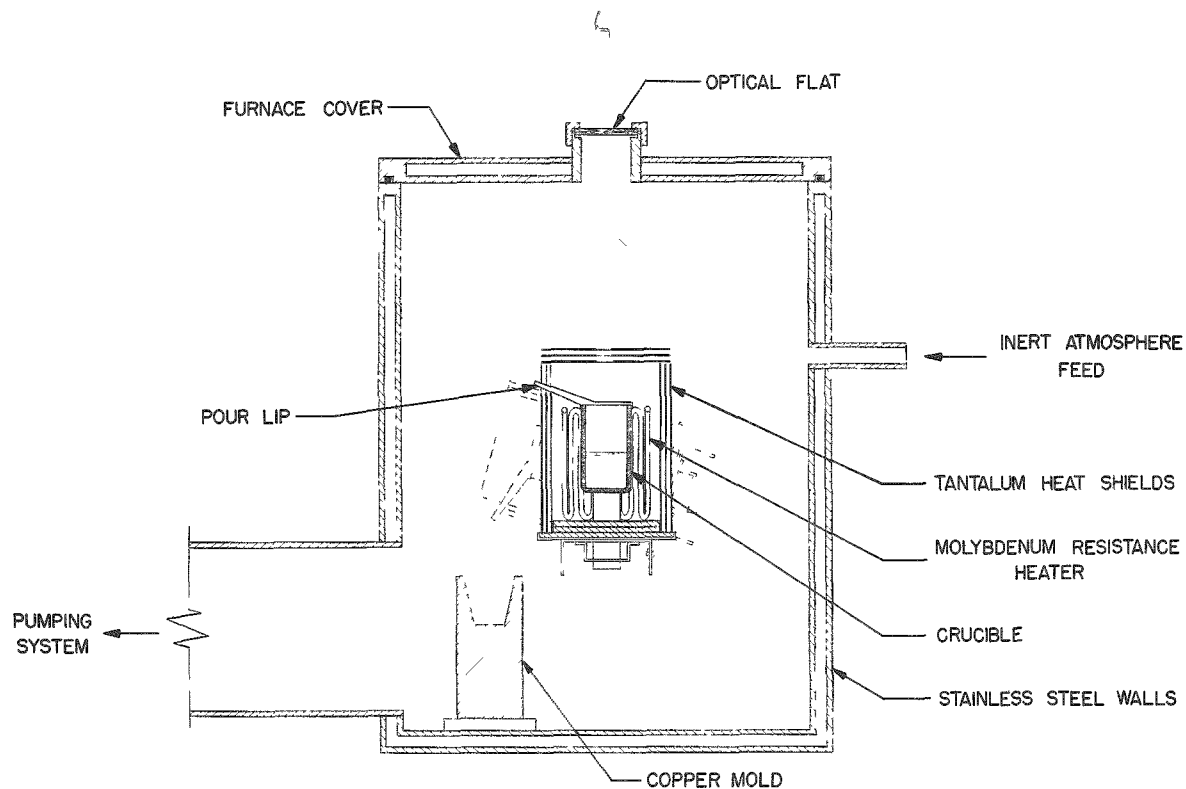
FIGURE 2

HIGH TEMPERATURE MELTING AND CASTING FURNACE

Analyses were performed by conventional methods. The techniques used were: combustion for carbon; Kjeldahl for nitrogen; vacuum fusion for oxygen; and spectrophotometric determinations for aluminum, thorium, beryllium, and zirconium. The precision of all analyses, except that for aluminum, are estimated to be ± 10 per cent (relative). For aluminum this value was ± 3 per cent (relative) for reaction product studies and ± 5 per cent (relative) for kinetic studies.

III. RESULTS

A. Wettability

Wettability, because of its influence on the total area exposed to reaction, is one of the important rate-controlling variables in the reaction of a liquid with a porous material.

Figure 3 is a photograph of a sessile drop of uranium on a zirconia plaque taken one minute after melting. The geometry of the

button before melting was found to have no effect on the final shape of the drop. Observations from eleven wettability experiments, each conducted in vacuum and helium atmosphere, are recorded in Table 2. The contact angle for liquid uranium on each of the five ceramics tested was approximately 135°. Contact angles slightly greater than 90° were measured for ruthenium and molybdenum alloys on alumina. The initial wettability of the various ceramics by uranium will therefore not be a significant factor in causing variations in their corrosion rates. Only in the case of alumina with the alloys mentioned is wettability expected to be a possible source of accelerated corrosion.

Uranium Drop

Zirconia Plaque
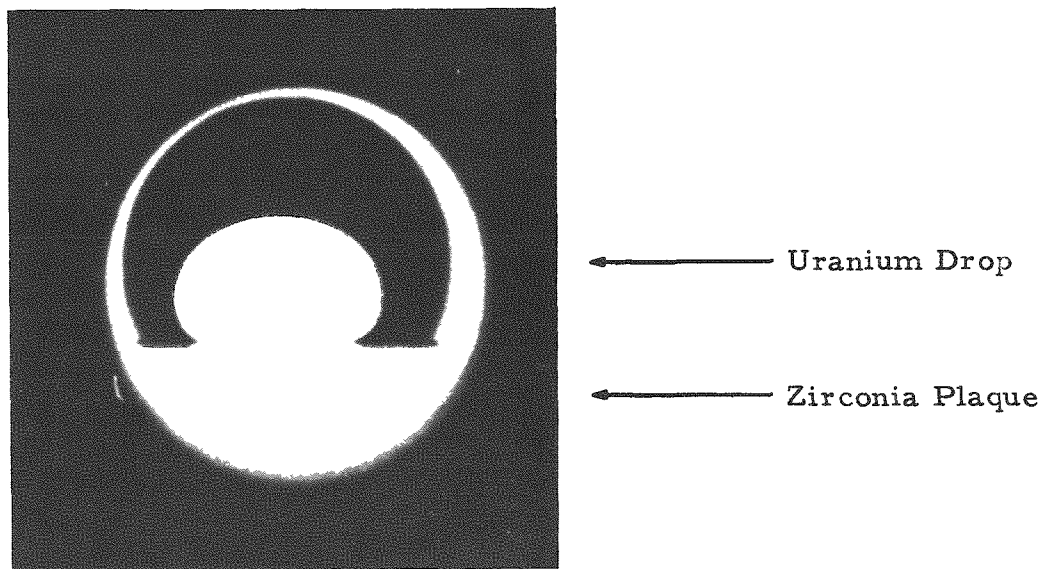
FIGURE 3

PHOTOGRAPH OF A SESSILE DROP OF URANIUM
STABILIZED ZIRCONIA 1225 C

Table 2

WETTING OF CERAMIC OXIDES BY URANIUM
AND URANIUM ALLOYS

Oxide	Metal	Wettability
Alumina	U	Non-Wetting
Alumina	U-4 w/o Mo, U-4.6 w/o Ru	Nearly Wetting
Magnesia	U	Non-Wetting
Zirconia	U	Non-Wetting
Zirconia	U-4 w/o Mo, U-4.6 w/o Ru	Non-Wetting
Beryllia	U	Non-Wetting
Thoria	U	Non-Wetting
Thoria	U-4 w/o Mo, U-4.6 w/o Ru	Non-Wetting

B. Products of Reaction and Mechanisms

    1. Alumina

        When uranium is melted on dense recrystallized alumina the plaque is undercut, but not discolored, by reaction or by penetration of its pores by liquid metal. A uniformly thick reaction layer covering the entire area in contact with metal is formed. Figure 4 is a photomicrographic section through the contact layers which illustrates undercutting of the plaque. In various experiments the depth of undercutting varied from one-third to slightly greater than the thickness of the reaction layer formed. A highly polished section of the detached reaction layer is shown in Figure 5. Irregularities observed were voids and occluded uranium. Powder samples of the layer from a typical melt on alumina were examined by X-ray diffraction. A face-centered cubic lattice was identified with an a_0 parameter of 5.470 ± 0.001 Å. This structure has been identified as $UO_{2.0}$.

        The source of the dross-forming oxygen was established from analyses for aluminum and oxygen in the uranium and in the uranium dioxide formed. Concentrations of aluminum and oxygen in these phases are shown in Table 3. It is evident that the small amount of aluminum (less than 3.8 per cent) found in the reaction layer is relatively insignificant. It may be present as minute particles of alumina or as aluminum in the occluded metal. From the phase diagram of the system it is known that solid solution of alumina in urania does not occur.[3] On the other hand, more than 96 per cent of the aluminum recovered was found in the uranium and less than 2 per cent of the oxygen recovered was found there. Comparison of the empirical formulas calculated from total recovered aluminum and oxygen, $Al_2O_{2.60}$ and $Al_2O_{2.68}$, with the theoretical ratio of the elements in alumina is evidence that within combined errors of measurement the alumina is the sole oxidant in these experiments. It may be concluded that the equation

$$U \, (\ell) + 2/3 \, Al_2O_3 \, (s) \longrightarrow UO_2 \, (s) + 4/3 \, Al \, (\text{sol. in U})$$

describes the over-all corrosion reaction quantitatively when the experiment is conducted in a helium atmosphere. When the experiment was conducted in vacuum, weight loss measurements gave evidence that a gaseous product, presumably Al_2O, was also formed.

    2. Magnesia

        When uranium is melted on high-purity magnesia the interfacial reaction zone was similar to that formed on alumina (Figure 6). Undercutting proceeds in the same way and a urania reaction layer containing many fissures and voids is formed. With high-density magnesia plaques no discoloration of the ceramic was seen adjacent to the reaction

FIGURE 4

UNDERCUTTING OF CERAMIC
URANIUM-ALUMINA   2 HR AT 1200 C

Original
Interface →

← Reaction
Layer
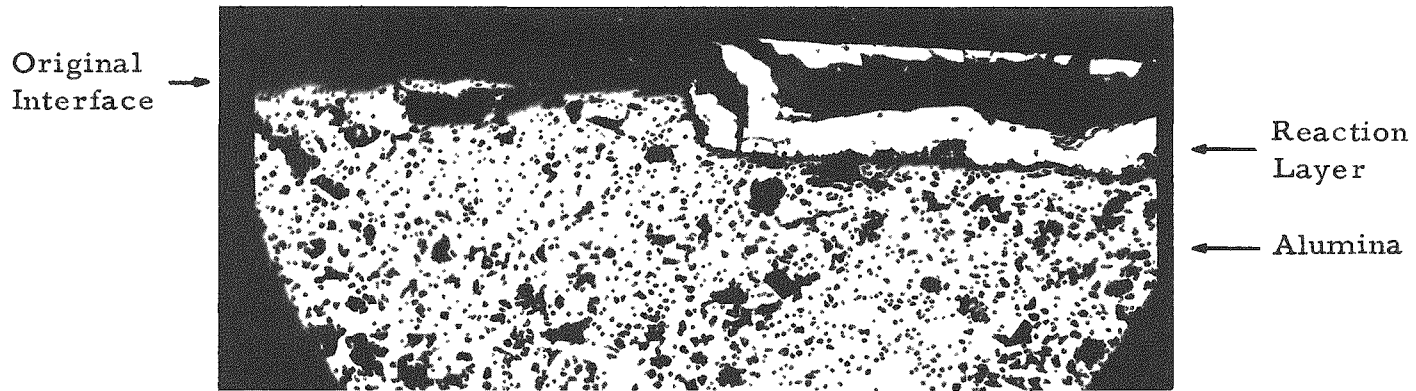
← Alumina

Magnification 100x

FIGURE 5

PHOTOMICROGRAPH OF DETACHED REACTION LAYER
URANIUM-ALUMINA   2 HR AT 1300 C

Ceramic
← Contact
Surface

~170
Microns

Metal
← Contact
Surface
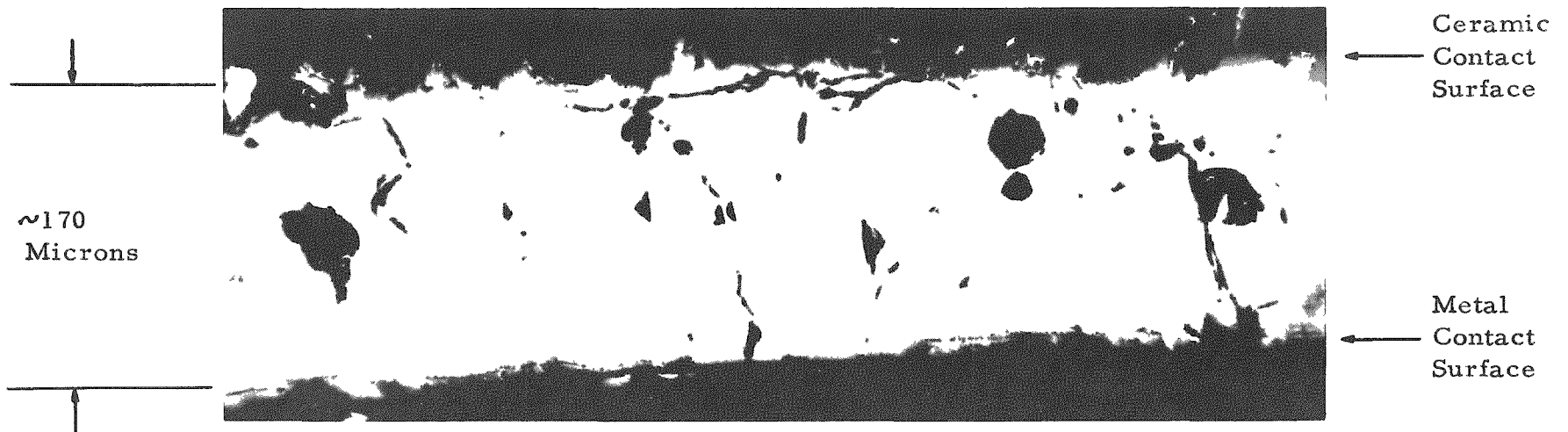
zone. With plaques of lower density, however, there was a slight discoloration due to metal flow into the pores. During these corrosion experiment- measurable weight losses due to volatilization of magnesium were obsc. ved. The evolution of this vapor left blow holes in rapidly frozen uranium ingots, but no measurable contamination by magnesium was found. Apart from the complete volatilization of the magnesium product the mechanisms of the reaction with alumina and with magnesia appear to be similar.

Table 3

DISTRIBUTION OF ALUMINUM AND OXYGEN FOR URANIUM-ALUMINA EXPERIMENTS AT 1300 C

Charge: Maximum impurity - 6 ppm oxygen, $<$14 ppm aluminum
Conditions: Helium atmosphere

Experiment	Element	Per Cent of Recovered Element[a] in Reaction Layer	Uranium Ingot	Formula Calculated
35	Aluminum	3.8	96.2	$Al_2O_{2.60}$
	Oxygen	98.4	1.6	
36	Aluminum	3.1	96.9	$Al_2O_{2.68}$
	Oxygen	99.5	0.5	

[a]Analytical Precision (relative): Aluminum, $\pm$ 3%; Oxygen, $\pm$ 10%

Reaction Layer

Magnification 250 x   Magnesia
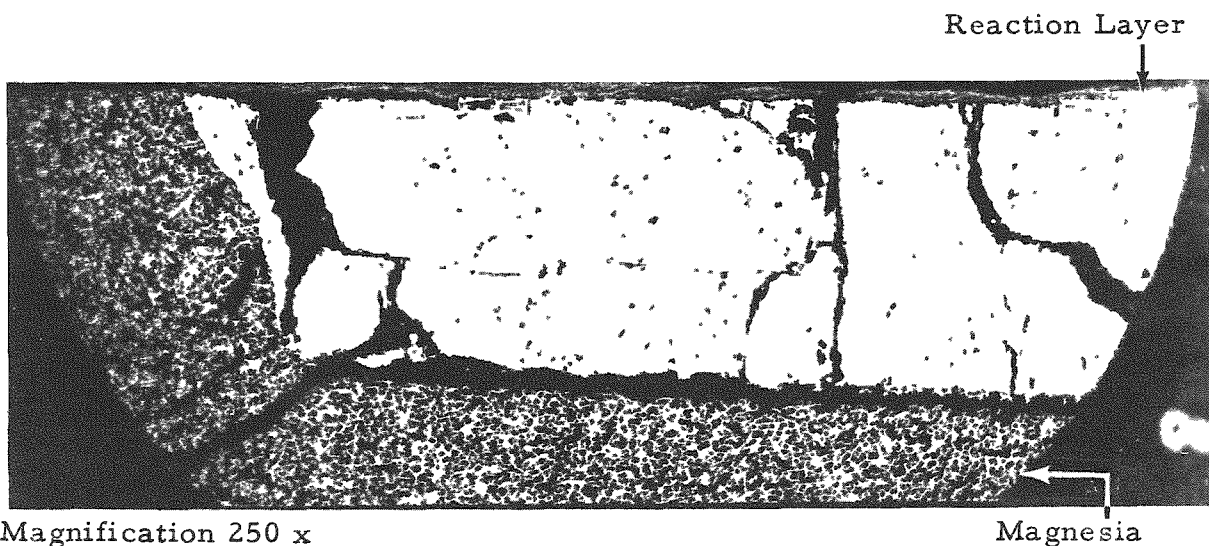
FIGURE 6

UNDERCUTTING OF CERAMIC URANIUM-MAGNESIA 3 HR AT 1225 C

3. Thoria, Beryllia, Lime-Stabilized Zirconia

Observations on the corrosion of thoria, lime-stabilized zirconia, and beryllia are offered together because of their many similarities. In each case the reaction product forms _above_ the original interface and undercutting is absent. Figure 7 shows the reaction layer formed above the original polished surface of a zirconia plaque. As the reaction proceeds the ceramic becomes progressively blackened. The blackening of thoria and zirconia plaques is pictured in Figure 8. The uranium button and the reaction layer have been removed for these photomicrographs.

Reaction Layer
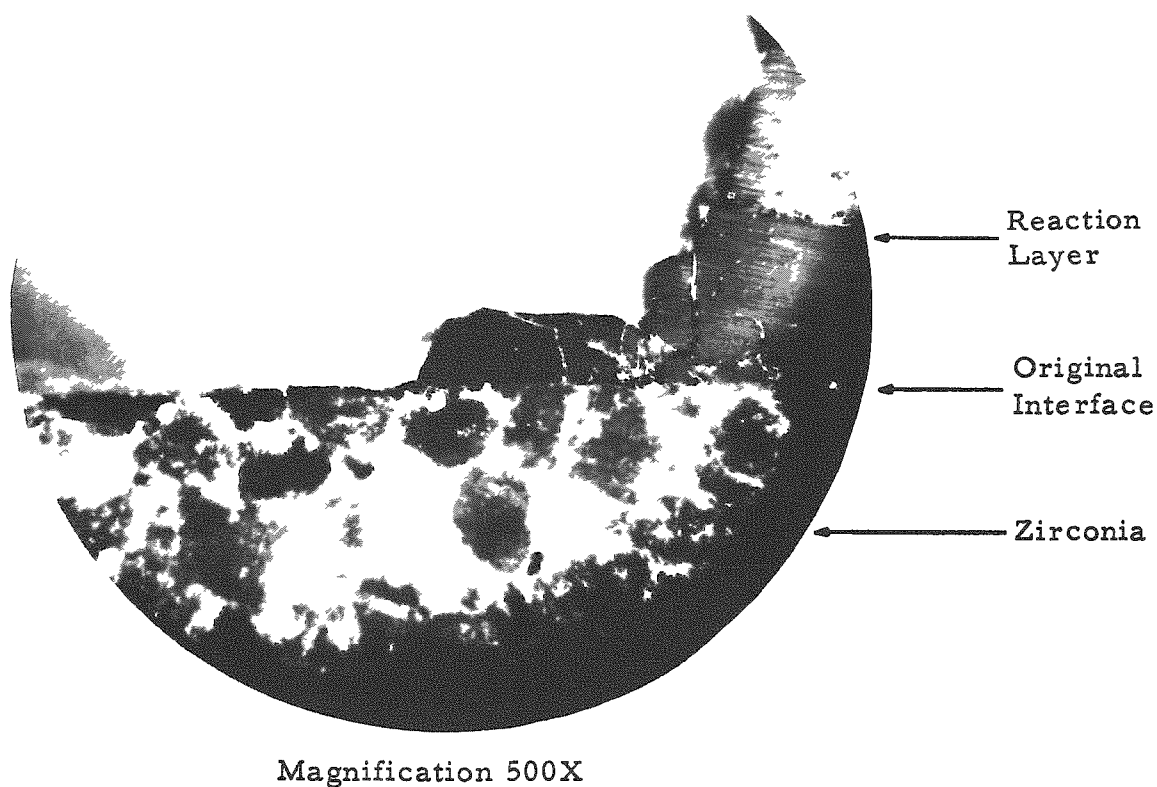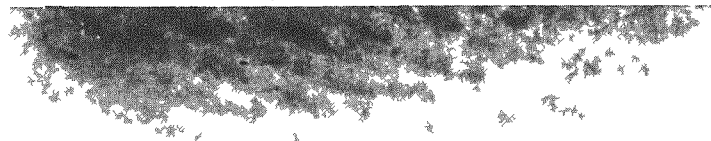
Original Interface

Zirconia

Magnification 500X

FIGURE 7

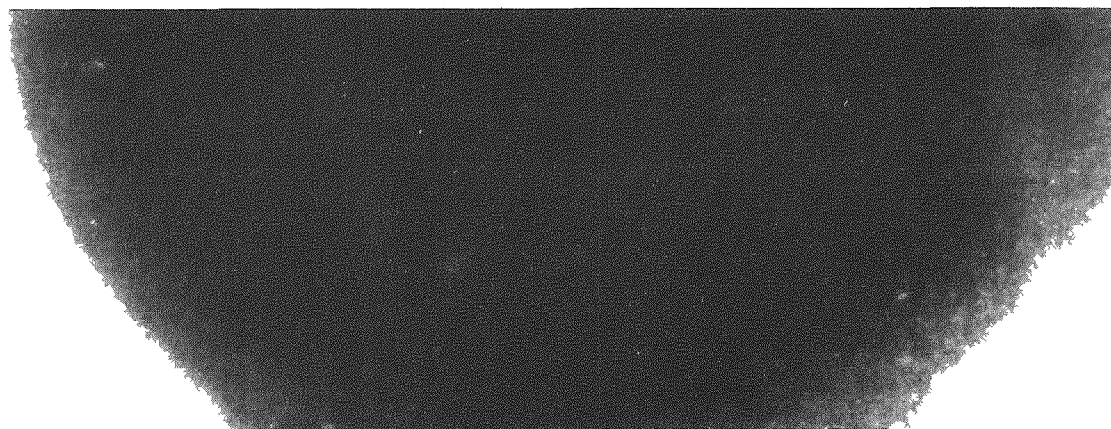REACTION INTERFACE URANIUM-STABILIZED ZIRCONIA 3 HR AT 1225 C

URANIUM-THORIA
1225 C

Uranium and Reaction Layer Removed

Magnification ~10X

URANIUM-STABILIZED ZIRCONIA
1225 C

Uranium and Reaction Layer Removed

Magnification ~10X

FIGURE 8
CROSS SECTIONS OF TYPICAL CERAMIC PLAQUES
SHOWING RADIAL BLACKENING

In one hour the blackening progressed distances of 8 and 30 millimeters, respectively, through the thoria and zirconia. The rate of travel was found to be independent of direction. Microscopic examinations of the unreacted and the blackened areas of these ceramics showed that the discoloration is associated with the accumulation of black material at the grain boundaries. The blackened areas, observed under ideal conditions of lighting and magnification, were seen to consist of two regions of different shade, separated by a sharp boundary, with the darker area immediately adjacent to the reaction zone. Chemical, radioactivity and fluorescence analyses all gave negative tests for the presence of trace uranium in the blackened areas. Heating a blackened plaque in air restored its original color, whereas heating in vacuum failed to do so. Thorium, zirconium, or beryllium was found to be dissolved in the uranium after the corrosion tests (see Section C and Table 6), but in each case the quantity was significantly less than the equivalent quantity of oxygen found as uranium dioxide.

Taken all together, these observations show that the corrosion of thoria, beryllia, and zirconia proceeds by preferential migration of oxide ions, particularly from grain boundaries in the ceramic, to the reacting interface, where formation of uranium dioxide takes place. The black intergranular materials are therefore identified with oxygen-deficient phases. Domagala and McPherson[4] examined the zirconium-oxygen system and found the lower stability limit for zirconia to be $ZrO_{1.7}$. The thorium-oxygen and beryllium-oxygen systems have not been quantitatively evaluated in the oxygen-deficient regions. It is further hypothesized that, in local regions where sufficiently extensive migration has occurred to attain the lower limit of stability of the oxygen-deficient phase, further loss of oxide ions results in formation of metal; the sharp inner boundary is presumed to define the limits of this reaction. All our observations are in accord with this proposed mechanism. Table 4 summarizes the observations and proposed mechanisms for the five refractory ceramic materials tested.

Table 4

REACTION OF URANIUM AND CERAMIC OXIDES
1175 TO 1330 C

Oxide	Discoloration	Interface	Reaction Products Found	Remarks
Al_2O_3	None	Undercut	Urania + aluminum in uranium solution	Stoichiometric reaction
MgO	None	Undercut	Urania + magnesium vapor	Stoichiometric reaction
ThO_2 ZrO_2 BeO	Progressive darkening; bleached by heating in air	Reaction layer above original interface	Urania + metal in uranium solution + oxide deficient substrates	Non-stoichiometric reaction; oxide ion migration mechanism

C. Kinetics of Reaction

Experimental results on the contamination of molten uranium by alumina, beryllia, thoria, and zirconia are reported here. Variations in ingot contamination were studied as a function of time, temperature, and contact area. In these tests the time during which the metal was molten, but not at a steady temperature, was held to a minimum by manipulation of the current through the molybdenum heater.

1. Alumina

Table 5 is a summary of the data from 26 corrosion experiments in recrystallized alumina. In Run 66 uranium was heated at a temperature approximately 15 degrees below its melting point for four hours in surface contact with the crucible. Since no aluminum pick-up by the metal was detected, it was concluded that in these experiments only molten uranium contributes to the corrosion reaction. The results of these kinetic studies are plotted in Figure 9 with the exception of three experiments at about 1145 C which will not be further considered because of the inadequacy of their number. Contamination expressed as milligrams of aluminum per square centimeter of crucible area contacted is plotted against total melt time for steady temperatures of 1200, 1260 and 1330 C. The straight lines representing the data were obtained by a least squares treatment after elimination of two runs of short duration in which gross contamination of aluminum was suspected. It was independently established that aluminum contamination is proportional to the crucible area contacted by the melt. This was done by an experiment at 1210 C in which the average crucible contact area (41 sq cm) of experiments reported in Table 5 was increased by a factor of 2.3. Ingot contamination was within 7.5 per cent of a value extrapolated from the kinetic data plotted in Figure 9.

It appears that corrosion proceeds at a constant rate after a small amount of initial attack. One may conclude that the uranium dioxide reaction layer formed is not protective.

An activation energy was calculated for the reaction after appropriate adjustment for the non-isothermal period in each run. The influence of these non-isothermal intervals, from three to sixteen minutes in duration, becomes negligible for runs of long duration, so the following technique was applied. The extent of reaction was calculated from equations of the lines for selected run durations. For each period of time the apparent activation energy was determined from an Arrhenius plot. These apparent activation energies are shown in Figure 10, from which the asymptotic value for the activation energy, 48.2 kcal/mole, may be deduced. The standard error of this value is estimated to be 0.6 kcal/mole.

Table 5

CORROSION OF ALUMINA BY MOLTEN URANIUM

Crucible: Morgan Triangle RR recrystallized alumina

Charge: 500 g high-purity uranium. Maximum impurity concentrations - 20 ppm carbon, 11 ppm nitrogen, 5 ppm oxygen, 33 ppm aluminum

Conditions: Helium atmosphere. Uranium charge liquated in crucible.

Experiment	Equilibrium Temp, C	Time at Equilibrium Temp, min	Time Molten, min	Crucible Area Contacted, sq cm	Corrosion,[a] mg Al/sq cm Contacted
66	1115	240	0	14.9	0.0
54	1145	39	40.3	40.4	0.89
75	1140	119	120.3	41.8	4.11
58	1140	175	176.3	39.1	4.66
50	1200	5	8.0	36.0	1.56
49	1200	24	30.0	36.3	2.30
56	1200	30	40.0	41.0	5.65
72	1200	36	42.0	39.4	3.80
52	1200	56	60.0	39.2	2.88
47	1200	114	119.0	36.9	4.38
1E	1200	117	120.0	43.7	5.25
48	1200	119	124.0	37.4	5.17
59	1200	170	176.0	38.9	7.80
53	1200	174	180.0	39.3	7.52
74	1200	235	240.0	40.6	7.81
51	1200	224	240.0	38.3	8.03
57	1260	25	35.0	43.9	7.70
96	1260	40	49.8	52.7	6.16
78	1260	110	120.8	42.2	8.46
60	1260	175	181.8	39.9	12.10
95	1260	228	239.8	50.7	14.98
55	1330	29	41.1	41.2	8.16
76	1330	26	41.1	41.0	10.36
94	1330	65	80.1	50.4	10.34
77	1330	108	124.1	41.8	19.17
61	1330	168	182.1	39.6	25.20

[a]Analytical precision (relative) Al, ± 5%; Measurement of area contacted, ± 3%.

FIGURE 9

CONTAMINATION OF URANIUM BY ALUMINUM

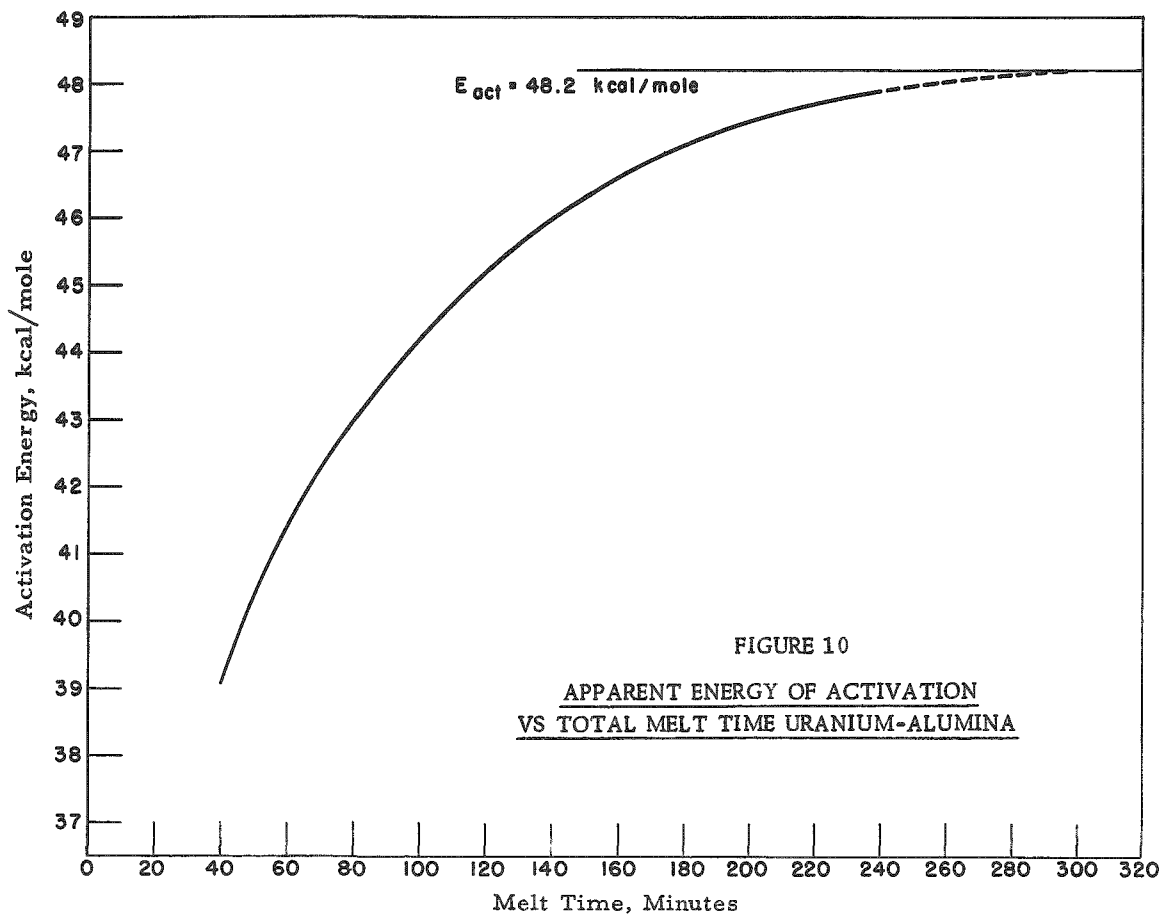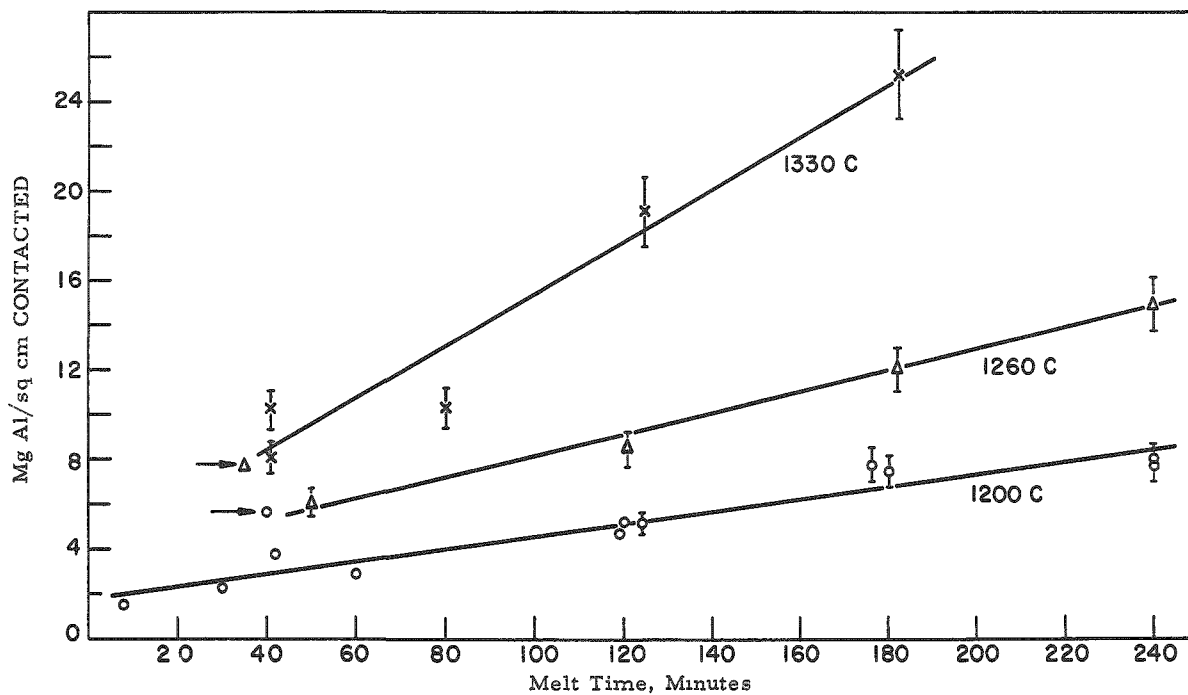Conditions: See Table 5

→ Values Eliminated

FIGURE 10

APPARENT ENERGY OF ACTIVATION
VS TOTAL MELT TIME URANIUM-ALUMINA

The addition of alloying elements frequently changes corrosion behavior in a drastic manner. The contamination of alloyed uranium by aluminum is compared with the contamination occurring with unalloyed uranium under similar conditions in Figure 11. Base corrosion rates for uranium were taken from plots of the relevant kinetic studies. The corrosion rate is increased with the addition of small amounts of zirconium, thorium, or molybdenum to the uranium. For the latter element the increase by a factor of 3.4 can be ascribed, at least in part, to the greater wettability of the ceramic (see Table 2). The observed decrease in aluminum pick-up when either carbon or the two rare earth elements Ce and La were added can be correlated with the results of an examination of the reaction layers formed. Analysis of the reaction layer from the carbon-alloy experiment showed a five-fold increase in carbon content over the charged material. It is probable that uranium carbide coats the crucible wall and thereby lessens the attack on the alumina. With the cerium alloys, a dense, yellowish, crystalline layer of cerium oxide was found between the crucible wall and a typical uranium dioxide layer. The rapid preferential oxidation of the solute cerium at the alumina crucible wall evidently forms a semi-protective barrier which retards the corrosion process. Lanthanum is assumed to behave in a manner similar to cerium.
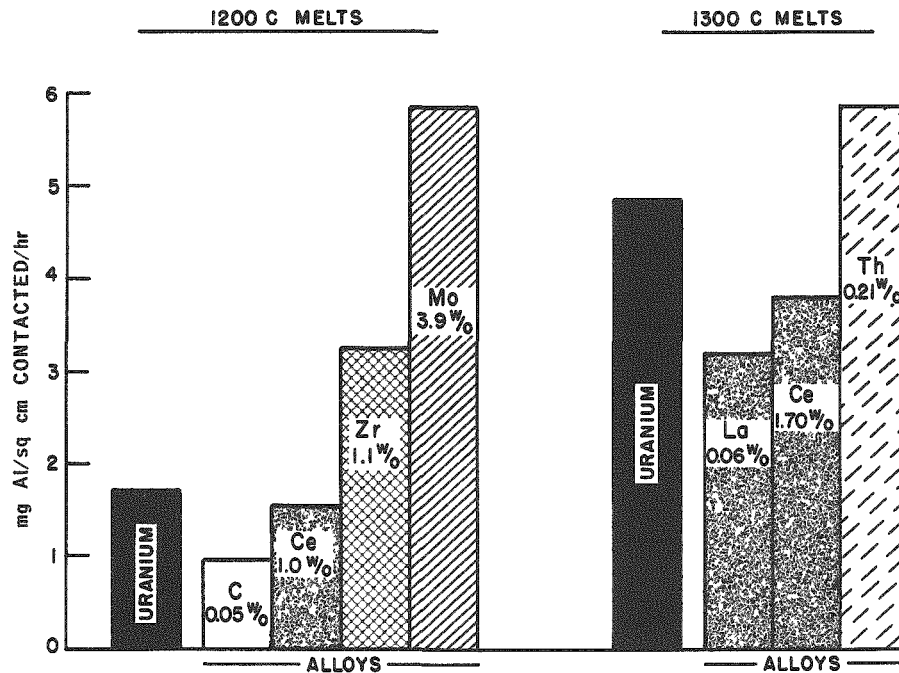

FIGURE 11

TYPICAL CONTAMINATION OF URANIUM ALLOYS BY ALUMINUM

Crucible: Morgan Triangle RR recrystalized alumina
Charge: Maximum impurity-39 ppm carbon, 5 ppm nitrogen, 11 ppm oxygen
Conditions: Helium atmosphere

2. Thoria and Beryllia

When uranium was melted in thoria or beryllia crucibles (thermodynamically more stable than alumina) contamination of the uranium by thorium or beryllium occurred at a much slower rate and is reported in micrograms per square centimeter of area in contact with the melt in Table 6.

Table 6

CONTAMINATION OF URANIUM BY BERYLLIUM AND THORIUM

Charge: Maximum impurity - 39 ppm carbon, 10 ppm nitrogen, 11 ppm oxygen

Conditions: Helium atmosphere; uranium charges liquated in crucibles

Experiment	Crucible	Melt Conditions		Contamination, μg/sq cm Contacted[a]	
		Nominal Temp, C	Total Time, min		
86	BeO (Slip Cast)	1200	120	13	
133	BeO (Slip Cast)	1300	150	23	
107	BeO (Slip Cast)	1330	62	17	
106	BeO (Slip Cast)	1330	152	62	Be
108	BeO (Slip Cast)	1330	242	133	
134	BeO (Slip Cast)	1330	300	153	
135	BeO (Slip Cast)	1330	360	221	
83	ThO_2 (Slip Cast)	1200	120	<5	
87	ThO_2-Coated Al_2O_3	1205	120	<5	
103	ThO_2-Coated Al_2O_3	1300	60	<10	Th
105	ThO_2-Coated Al_2O_3	1306	152	25	
102	ThO_2-Coated Al_2O_3	1300	241	64	

[a]Analytical Precision (relative): Be and Th, ± 10%; Measurement of area contacted, ±3%.

The contamination at 1200 C was found to be near the lower limit of analytical determination; hence, a higher temperature was chosen for the rate study. These experimental results are plotted in Figure 12. For both elements the data show that contamination increases in a non-linear manner, the rate increasing with time up to 4 hr for thoria and 6 hr for beryllia.
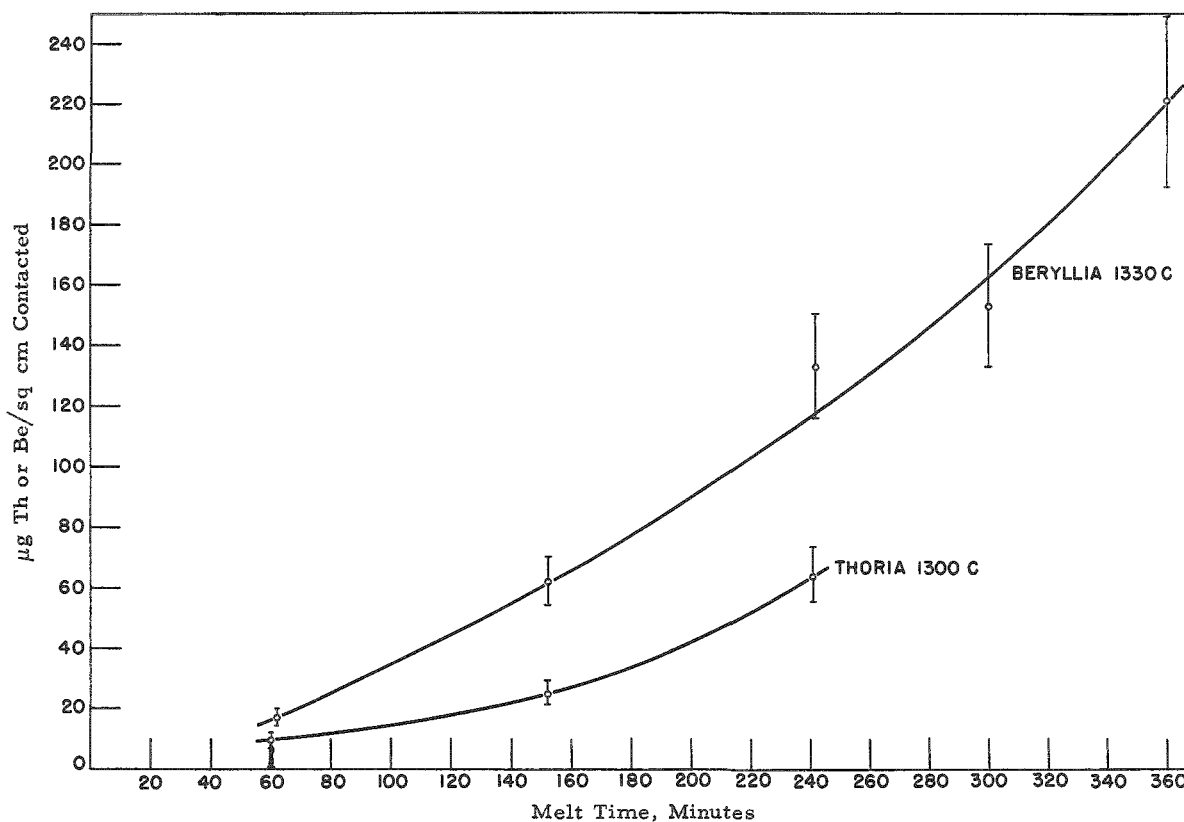
FIGURE 12

CONTAMINATION OF URANIUM BY BERYLLIUM AND THORIUM

Conditions: See Table 6

The non-linear increase of metal contamination in the melt can be simply explained on the basis of two assumptions: (1) the instantaneous rate of metal pickup in the melt is proportional to its concentration at the reacting interface, and (2) the rate of reaction of the melt with oxygen at the reacting interface is greater than the rate of reaction with the metal. The second assumption is, of course, already implicit in the earlier discussion of the mechanism of formation of the suboxide phases. It is then readily seen that the concentration of metal at the reacting interface increases with time.

The contamination of uranium alloys by beryllium and thorium is compared with the contamination of unalloyed uranium in Figure 13. Corrosion rates for the uranium were again taken from relevant kinetic studies. Although some increase in reaction rate was noted when uranium alloys containing small amounts of ruthenium or molybdenum

were melted in thoria, the same alloys when melted in beryllia showed little change in reaction rate from the value of pure uranium. With cerium alloy in beryllia, however, an increase in rate by a factor of about 20 was observed. Data on these experiments are too fragmentary to permit generalization of the variations noted.
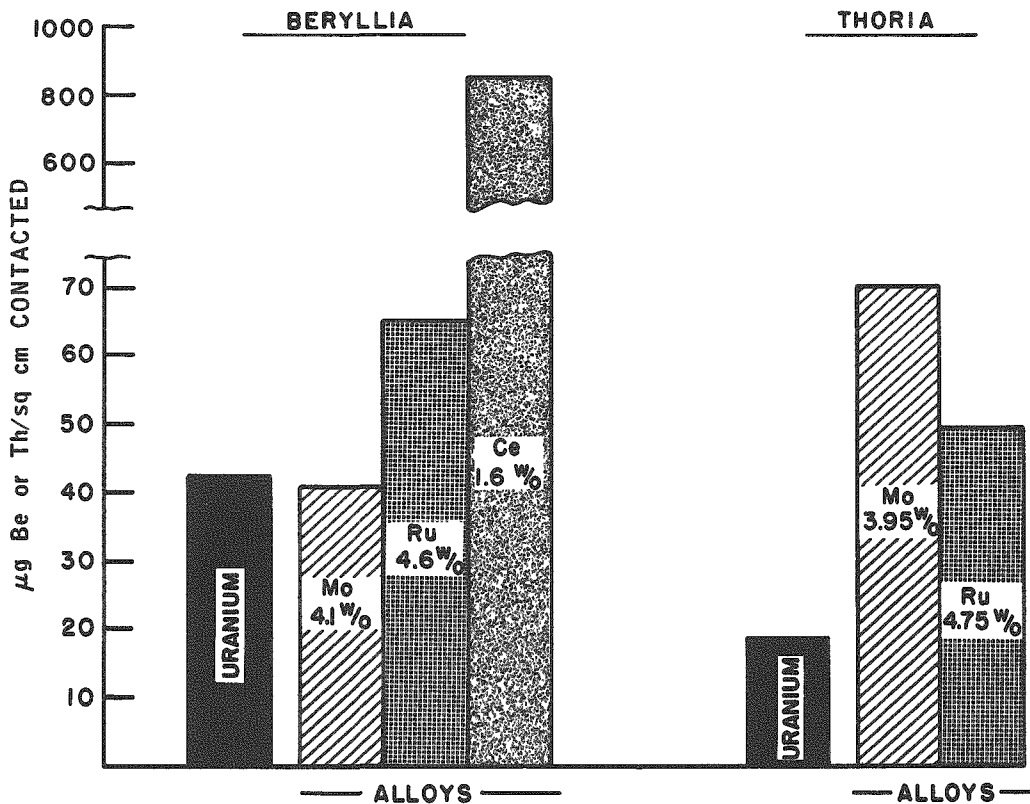

FIGURE 13

TYPICAL CONTAMINATION OF URANIUM ALLOYS BY BERYLLIUM AND THORIUM
1300 C - 2 HOURS

Crucibles: Slip cast
Charge: Maximum impurity - 39 ppm carbon, 5 ppm nitrogen, 11 ppm oxygen
Conditions: Helium atmosphere

3. Lime-Stabilized Zirconia

An upper limit of 5 ppm zirconium was found in nine ingots obtained from uranium melts of 1 to 4-hr duration made in stabilized zirconia crucibles at 1200 to 1325 C. The inaccuracy of currently available methods for analysis of zirconium in uranium at very low concentrations

limits the value of these results. However, it is believed that metal contamination of uranium during melting in zirconia is not as great as in the comparable cases of melting in beryllia or thoria.

IV. SUMMARY

Qualitative and quantitative data from over 70 experiments have been summarized in this paper. The reaction mechanisms observed appear to fall into two categories. The oxides of thorium, beryllium and zirconium react by ionic diffusion to form an outward-growing interfacial layer. The kinetics are complex. Aluminum and magnesium oxides react in a straightforward manner in which the substrates are corroded away with the formation of a non-protective deposit of nearly pure uranium dioxide and an equivalent amount of either aluminum in uranium solution or volatilized magnesium. The latter process occurs with essentially constant velocity.

V. ACKNOWLEDGEMENTS

The authors wish to thank members of the Argonne National Laboratory who have contributed to this work: C. R. Cushing, D. Finucane, R. U. Sweezer, J. D. Schilb, for technical assistance and design; R. P. Larsen, L. E. Ross, R. W. Bane, for analyses; L. T. Lloyd for assistance in metallographic work; S. Siegel for x-ray diffraction photographs; and S. Rothman for numerous helpful discussions and criticisms.

VI. REFERENCES

1. H. M. Feder, N. Chellew, M. Ader, "Melt Refining of Uranium," Progress in Nuclear Energy, Pergamon Press, London, 1956, Vol. I.

2. F. H. Norton, W. D. Kingery, G. Economos, M. Humenik, Jr., "Study of Metal-Ceramic Interactions at Elevated Temperatures," Massachusetts Institute of Technology, NYO-3144 (February 1953).

3. W. A. Lambertson, M. H. Mueller, "Uranium Oxide Phase Equilibrium Systems," J. Am. Ceram. Soc., 36, 330 (1953).

4. R. F. Domagala, D. J. McPherson, "System Zirconium-Oxygen," J. of Metals, 200, 238 (1954).